I J C T A, 10(5) 2017, pp. 869-882

A Simple Control Scheme for DFIG to Improve its Steady State and Transient Performance

M. Venkateswarlu[*] and Y.P. Obulesu[**]

Abstract: In this proposed work Doubly Fed Induction Generator based wind turbine system Power can be controlled directly, by regulating the required rotor voltage to nullify the Active & Reactive Power errors in a certain time period. Which is directly determined depends on stator flux, rotor position, Active& Reactive Powers and also their errors. For this purpose it requires less power, so system design become simple and hence improving the transient performance. Further to simplify ac harmonic filter design maintains the converter switching frequency constantly. Simulation results for a 2MW Doubly Fed Induction Generator based wind turbine system acknowledge the strength and effectiveness of the proposed control scheme during changes in active and reactive powers, wind speed, and machine parameters etc.

Index Terms: Doubly Fed Induction Generator, Power Control directly, Active and Reactive Power, Constant Switching frequency and harmonic filter.

1. INTRODUCTION

In Renewable energy market Doubly Fed Induction Generator (DFIG)-based Wind Turbine scheme with Rectifiers became more popular. Because of their flexible speed, less cost of rectifiers and also four quadrants active and reactive power capacity, less power wastage compared to wind turbines with fixed speed Induction generators or fully-fed synchronous generators with full sized Rectifiers.

This Doubly Fed Induction Generator (DFIG)-wind turbine scheme's more convenient depends on either stator-flux [1], [2] or stator-voltage sloping vector control[3],in this scheme rotor current split into two components as active and reactive, active and reactive powers supervise with rotor current controller. Its presentation mainly depends on machine parameters i.e. stator and rotor resistance and inductance. Hence its presentation mortifies when the machine parameters quit from the values used control scheme.

A few years ago Induction machines direct torque Control (DTC) is developed, it is substitute to vector control method. DTC limits the machines parameters utilize and minimize vector control algorithms complexity. In This DTC method choosing voltage vectors from a table using stator flux and torque information to directly regulate machine torque and flux. Its presentation is poor at starting and at minimum speeds [4], but from the modified switching table to apply presented voltage vectors in suitable series [5], or analytical technique [6]. One more problem for DTC is Rectifier switching frequency deviation, this considerably confuse the power circuit design, customized DTC scheme introduce space vector modulation SVM have been used to obtain constant switching frequency [7].

Depends on control scheme principles power control directly (PCD) was developed for three phase pulse width modulation (PWM) rectifiers, most recently PCD of DFIG-base wind turbine system has been proposed [8]. In [9] the control system was based on expected rotor flux switching vectors were selected from minimized switching table using estimated rotor flux position, rotor flux errors and active power/torque. This rotor flux reference was calculated using the reactive power/power factor reference.

[*] Research Scholar, K.L. University
[**] Professor, K.L. University

In [10], PCD method based on the expected stator flux was proposed. Since the stator (network) voltage is harmonic free with fixed frequency, switching vectors were chooses from minimized switching table using the estimated stator flux position and active power, reactive power errors. Hence control system is very simple and machine parameters negligible.

This work proposes new PCD scheme for DFIG-based wind energy generation system for constant switching frequency and improved transient performance. This scheme directly computes the required rotor control voltage with each switching period, based on expected stator flux, the active and reactive powers and also their errors. This scheme describes to limit the rotor control voltage and further improve transient performance.

This Paper structured as Part III gives an overview of the original PCD scheme for DFIG control and Part IV explains the planned scheme. Simulation results for a 2MW DFIG generation system are presented in Part V to reveal the presentation of the planned control scheme. Finally conclusions are drawn in section VI.

2. PRINCIPLE OF DFIG POWER CONTROL DIRECTLY

Figure 1 shows the equivalent circuit of a DFIG Consider rotor reference frame $\alpha_r - \beta_r$ rotating at an angular speed of ω_r, from Figure 2 the stator voltage vector in the rotor frame is given as

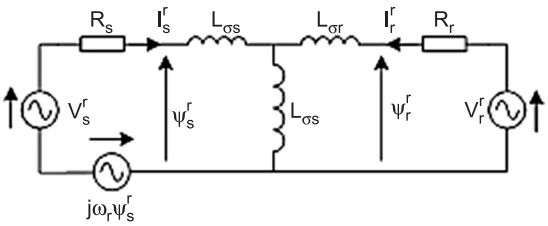

Figure 2: Equivalent circuit of a DFIG in the rotor reference frame

$$V_r^s = \mathrm{Rs}\, I_s^r + \frac{d\Psi_s^r}{dt} + j\omega_1 Y_s^r \tag{1}$$

And the stator and rotor flux are stated as

$$\Psi_s^r = L_s I_s^r + L_m I_r^r$$
$$\Psi_r^r = L_r I_r^r + L_m I_s^r \tag{2}$$

Where $L_s = L_{\sigma s} + L_m$ and $L_r = L_{\sigma r} + L_m$

Based on eq. (2), stator current is given as

$$I_s^r = \frac{L_r \Psi_s^r - L_m \Psi_r^r}{L_s L_r - L_m^2} = \frac{\Psi_s^r}{\sigma L_s} - \frac{L_m \Psi_r^r}{\sigma L_s L_r} \tag{3}$$

Where $\sigma = (L_s L_r - L_m^2)/L_s L_r$(leakage factor) Referred [20], Stator Active and Reactive power inputs from the network can be calculated as

$$P_s - jQ_s = \frac{3}{2} V_s^r \times \hat{I}_s^r \tag{4}$$

Assume Stator resistance neglected and the network voltage is constant, Stator flux magnitude $|\Psi_s|$ and the angular speed ω_1 remains constant [19]. By Substitute eq. (1) and (3) in eq. (4) gives the Stator Active and Reactive power inputs [19]:

$$P_s = -k_\sigma \omega_1 |\Psi_s||\Psi_r| \sin\theta \text{ yield}$$

$$Q_s = k_\sigma \omega_1 |\Psi_s| \left(|\Psi_r| \cos\theta - \frac{L_r}{L_m} |\Psi_s| \right) \quad (5)$$

Where $k_\sigma = 1.5\, L_m/(\sigma L_s L_r)$ and θ is the angle between stator flux vectors, and rotor as shown in Figure 3. By differentiate eq. (5) we get the following results:

$$\frac{dP_s}{dt} = -k_\sigma \omega_1 |\Psi_s| \frac{d\left(|\Psi_r| \sin\theta\right)}{dt}$$

$$\frac{dQ_s}{dt} = k_\sigma \omega_1 |\Psi_s| \frac{d\left(|\Psi_r| \cos\theta\right)}{dt} \quad (6)$$

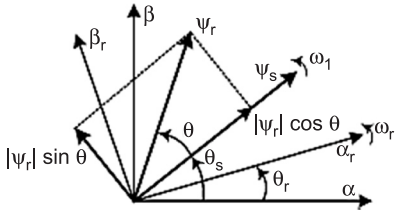

Figure 3: Stator and rotor flux vectors in stationary and rotor reference frames

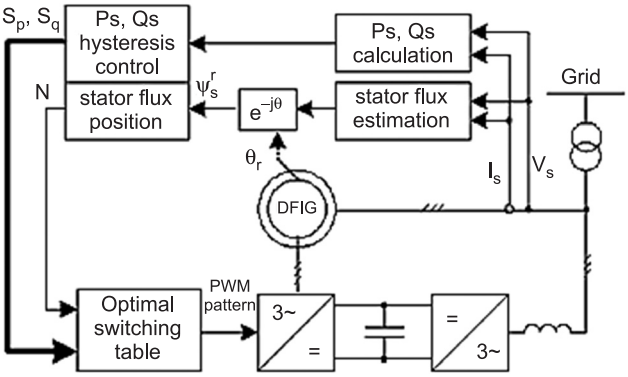

Figure 4: Schematic of the original DPC control strategy [19].

As $|\Psi_s|$ and ω_1 remains constant, eq. (6) designates the distinction of active and reactive power can be controlled by changing the rotor flux components $|\Psi_r| \sin\theta$ and $|\Psi_r| \cos\theta$ respectively. The relations between $|\Psi_r| \sin\theta$ and $|\Psi_r| \cos\theta$, the stator flux the rotor flux can be seen in Figure 3.

From Figure 2, if neglecting the rotor resistance, the rotor flux changes in the rotor reference frame can be approximated as

$$\frac{d\Psi_r^r}{dt} = V_r^r - R_r I_r^r \approx V_r^r \quad (7)$$

Eq. (7) designates the variation in the rotor flux can directly controlled by the applied rotor voltage, and its speed is relative to the voltage vector magnitude. If the stator flux situation is recognized, the effect of every voltage vector on the variation of the rotor flux $|\Psi_r| \sin\theta$ and $|\Psi_r| \cos\theta$ can be obtained. Therefore,

According eq. (6), the effect of every voltage vector on active and reactive power deviation can be designed. Then best switching table can be approved to give the most efficient rotor voltage vector to decrease the power errors.

The array of the PCD scheme planned in [19] as shown in Figure 4. Active and Reactive powers Hysteresis control in every sampling time is achieved by selecting and applying the best rotor voltage vector. In order to assurance the efficient power control, the sampling frequency must be adequately lofty, normally tens of kilohertz range.

The Rectifiers switching frequency highly depends on the working circumstances such as the Active and Reactive Powers, hysteresis bandwidth, rotor slip etc., and vary knowingly [19]. Hence, it is tough to calculate the rotor-side converter's power loss and loading conditions, and suitable cooling system design. Since the variable switching frequency, harmonics in the stator currents also vary according to the working circumstances. The AC filter has knowingly complex plan, since it has to absorb broadband frequency components to prevent their entering the network.

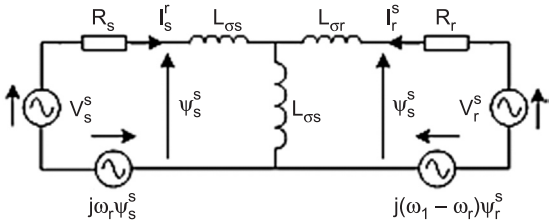

Figure 5: Equivalent circuit of a DFIG in the synchronous *d-p* reference frame

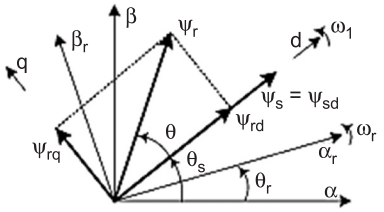

Figure 6: Stator and rotor flux vectors in the synchronous *d-p* frame

3. PROPOSEDPCDSCHEME

A. Demonstration of DFIG in the Synchronous Reference Frame

Figure 5 shows the DFIG equivalent circuit in the synchronous *d-q* frame, rotating with ω_1 speed. The *d*-axis of the synchronous frame is fixed to the stator flux, as shown in Figure 6.

From Figure 5 the Stator voltage vector in the synchronous *d-q* reference frame is given as

$$V_s^s = RS\, I_s^s + \frac{d\Psi_s^s}{dt} + j\omega_1 \Psi_s^s \tag{8}$$

Stator flux magnitude and rotating speed are constant under balanced ac voltage supply. Therefore in the synchronous *d-q* frame the stator flux maintains a constant value. Thus $\Psi_s^s = \Psi_{sd}$;

$$\frac{d\Psi_s^s}{dt} = 0 \tag{9}$$

Substitute the eq. (9) in eq. (8) and neglecting the voltage drop across the stator resistance, we get

$$V_s^s = j\omega_1 \Psi_s^s = j\omega_1 \Psi_{sd} \tag{10}$$

This equation (10) same as eq. (3), i.e., the stator current in the synchronous *d-q* frame is given as

$$I_s^s = \frac{L_r \Psi_s^s - L_m \Psi_r^s}{L_s L_r - L_m^2} = \frac{\Psi_s^s}{\sigma L_s} - \frac{L_m \Psi_r^s}{\sigma L_s L_r} \tag{11}$$

Thus, the Stator Active and Reactive power inputs can be planned as

$$\begin{aligned} P_s - jQ_s &= \frac{3}{2} j\omega_1 \psi_{sd} \times \left(\frac{\Psi_s^s}{\sigma L_s} - \frac{L_m \Psi_r^s}{\sigma L_s L_r} \right) \\ &= \frac{3}{2} j\omega_1 \psi_{sd} \times \left[\frac{\Psi_{sd}}{\sigma L_s} - \frac{L_m (\psi_{rd} - j\psi_{rq})}{\sigma L_s L_r} \right] \\ &= k_\sigma \omega_1 \left[-\psi_{sd} \psi_{rq} \times j\psi_{sd} \left(\frac{L_r \psi_{sd}}{L_m} - \psi_{rd} \right) \right] \end{aligned} \tag{12}$$

Splitting eq. (12) into real and imaginary parts as

$$\begin{aligned} P_s &= -k_\sigma \omega_1 \Psi_{sd} \Psi_{rq} \\ Q_s &= k_\sigma \omega_1 \psi_{sd} \left(\psi_{rd} - \frac{L_r}{L_m} \psi_{sd} \right) \end{aligned} \tag{13}$$

As the stator flux stable, from eq. (13), the Active and Reactive power changes over a constant time (T_s) are given by

$$\begin{aligned} \Delta P_s &= -k_\sigma \omega_1 \Psi_{sd} \Delta \Psi_{rq} \\ \Delta Q_s &= k_\sigma \omega_1 \Psi_{sd} \Delta \Psi_{rq} \end{aligned} \tag{14}$$

Equation (14) shows that the stator active and reactive power changes are determined by the changes of the rotor flux components on the *d-q* axis i.e., $\Delta\Psi_{rd}$ and $\Delta\Psi_{rq}$ respectively.

B. Control of Active and Reactive Power

The planned control of Active and Reactive powers obtain the necessary rotor voltage, it will decrease the active and reactive power errors to zero during a constant sampling time period T_s. Then A PWM modulator is used to produce the applied rotor voltage for the sampling time period T_s. At the starting of sampling time (T_s), the active reactive power errors are determined as

$$\begin{aligned} \Delta P_s &= P_s^2 - P_s \\ \Delta Q_s &= Q_s^2 - Q_s \end{aligned} \tag{15}$$

From eq. (14), in order to decrease the power errors as shown eq. (15) to zero, the rotor flux changes in the *d-q* axis must as follow

$$\begin{aligned} \Delta \Psi_{rd} &= -\frac{\Delta P_s}{k\sigma\omega_1 \Psi_{sd}} \\ \Delta \Psi_{rd} &= \frac{\Delta Q_s}{k\sigma\omega_1 \Psi_{sd}} \end{aligned} \tag{16}$$

As shown in Figure 5, in the synchronous *d-q* reference frame, the rotor flux is given by

$$\frac{d\Psi_r^s}{dt} = V_r^s - R_s I_r^s - J(\omega_1 - \omega_r)\Psi_r^s \tag{17}$$

Neglect the rotor resistance, within the sampling time (T_s) the changes of rotor flux in the *d*-and *q*-axis are given by

$$\Delta\Psi_{rd} = V_{rd}T_s + \omega_s\Psi_{rq}T_s$$
$$\Delta\Psi_{rq} = V_{rq}T_s - \omega_s\Psi_{rd}T_s \quad (18)$$

Where $\omega_s = (\omega_1 - \omega_r)$ is the slip frequency.

By adding eq. (16) and eq. (18) within the sampling time (T_s) the required rotor voltage to eliminate the power errors in the *d-q* reference frame is determined as

$$V_{rd} = \frac{1}{T_s}\frac{\Delta Q_s}{k\sigma\omega_1\Psi_{sd}} - \omega_s\Psi_{rq}$$
$$V_{rq} = \frac{1}{T_s}\frac{-\Delta P_s}{k\sigma\omega_1\Psi_{sd}} + \omega_s\Psi_{rq} \quad (19)$$

The Rotor flux in the *d-q* frame can be determined using a method, which is shown in eq. (2). How ever its exactness could be affected by the variation of L_m as will be discussed later. An another method is based on eq. (13) as

$$\Psi_{rd} = \frac{Q_s}{k\sigma\omega_1\Psi_{sd}} + \frac{L_r}{L_m}\Psi_{sd}$$
$$\Psi_{rq} = \frac{-P_s}{k\sigma\omega_1\Psi_{sd}} \quad (20)$$

Substituting eq. (20) into (19) results in the required rotor voltage in the *d-q* reference frame

$$V_{rd} = \frac{1}{T_s}\frac{\Delta Q_s}{k\sigma\omega_1\Psi_{sd}} + \omega_s\frac{P_s}{k\sigma\omega_1\Psi_{sd}}$$
$$V_{rq} = \frac{1}{T_s}\frac{-\Delta P_s}{k\sigma\omega_1\Psi_{sd}} + \omega_s\left(\frac{Q_s}{k\sigma\omega_1\Psi_{sd}} + \frac{L_r}{L_m}\psi_{sd}\right) \quad (21)$$

In eq. (21) first terms on the right hand side decrease the power errors while second terms recompense the rotor slip that causes dissimilar rotating speeds of the stator and rotor flux.

C. Voltage Limit of Rotor Output and PWM

In normal operation, the required rotor control voltages conquer the voltage limit of rotor side converter. While during intransient condition, most changes of active and/or reactive power references can result in heavy power errors in one sampling time T_s. Therefore, the rotor voltage V_{rd} and V_{rq} should be reduced to improve the transient response. In DFIG, the peak output voltage of the rotor side converter is generally within the range of 30% of the stator voltage. In the large active power errors, determined V_{rq} is conquer the voltage range, while V_{rd} remains within the range. Generally voltage components are scaled proportionately. However the scaling of V_{rd} in case could result in reactive power control being temporarily lost. The approach altered here maintains V_{rd} and V_{rq} according to the maximum voltage range such that reactive power remains controlled while active power driven towards the desired value. This method can be represented as

$$V'_{rd} = V_{rd}$$
$$V'_{rq} = \text{sign}\,(V_{rq})\sqrt{V^2_{r\max} - V^2_{rd}} \quad (22)$$

Where $V_{r\,max}$ is the peak voltage of the rotor side converter can generate.

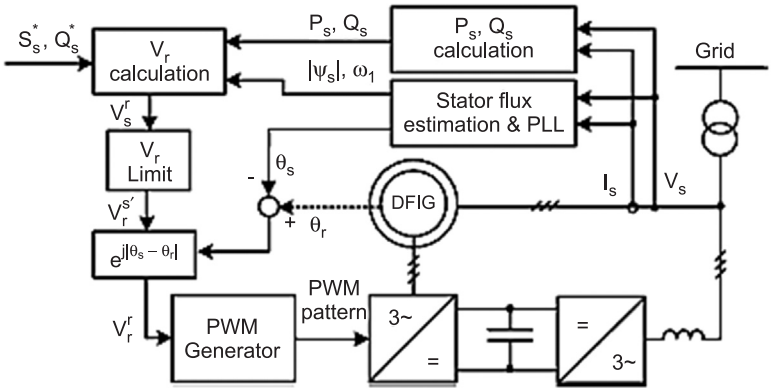

Figure 7: Schematic of the proposed DPC for a DFIG system

But during reactive power steps when V_{rq} remains unaffected while V_{rd} is scaled Within the sampling time, if simultaneous step changes of active and reactive powers cause both V_{rd} and V_{rq} to conquer the voltage range, V_{rd} and V_{rq} are scaled proportionately as

$$V'_{rd} = V_{rd} \frac{V_{r\,max}}{\sqrt{V_{rd}^2 + V_{rq}^2}}$$

$$V'_{rq} = V_{rq} \frac{V_{r\,max}}{\sqrt{V_{rd}^2 + V_{rq}^2}} \tag{23}$$

In the synchronous reference frame, if the desired rotor output voltage is reach, it should be changed to rotor $\alpha_r - \beta_r$ reference frame using the following equation.

$$V_r^r = V_r^s e^{j(\theta s - \theta r)} \tag{24}$$

The required rotor voltage in the rotor frame can produce switching signals to the rotor side converter using SVM [21] or sinusoidal PWM [22] whose switching frequency is fixed continually at $1/(2T_s)$. For this rotor converter switching frequency is within a few KHz, and therefore, the proposed PCD sampling frequency is within a few KHz range.

D. System Implementation

From eq. (21) and eq. (24), determine the required rotor voltage, active and reactive powers and their errors, from the stator flux, rotating speed and the rotor angle.

The stator instant active and reactive powers can be directly determined from the measured stator voltage and current. With stationary reference frame, the stator flux is determined using the following:

$$\Psi_s = \int (V_s - R_s I_s)\, dt \tag{25}$$

Figure 7 shows the planed PCD schematic. The three phase stator voltage and currents are measured and changed into the stationary α–β reference frame. The stator active and reactive powers are determined and the stator flux is estimated. A phase-locked loop (PLL) is, used to determine the stator flux angle θs and its rotating speed ω_1, then rotor *d-q* control voltage references are, determined with eq. (21), they are passed to the voltage limiter and changed to the rotor frame using the rotor angle i.e., obtained by shaft encoder. Finally PWM switching pattern is generated and used to control the rotor side converter.

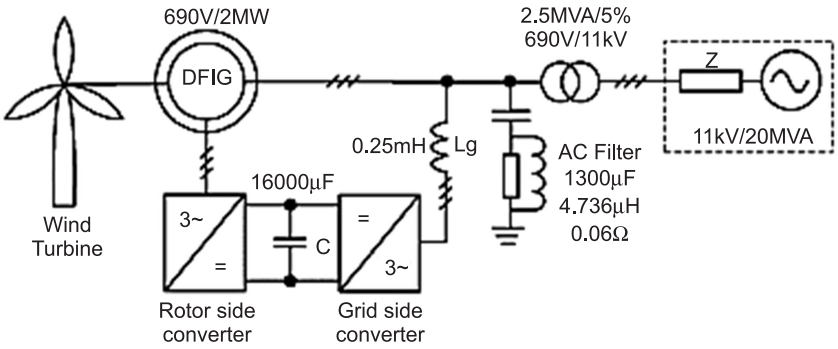

Figure 8: Schematic of the simulated system

E. Parameters Magnitude Changing Effect on System Performance

Guessing of Stator flux must require awareness about stator resistance that has negligible effect on system performance [19]. Using eq. (21), rotor voltage calculation accuracy is mainly influenced by the constant $k\sigma$ and the ratio of inductance L_r/L_m that are determined by the stator and rotor seepage and mutual inductance. Due to the seepage flux magnetic path is mainly air; the seepage inductance deviation during operation is immaterial. However, mutual inductance deviation needs to be considered due to possible deviation of the stator magnetic permeability and rotor core under different operating conditions. As described in Appendix A, considering relatively small seepage inductance $L_{\sigma s}$ and $L_{\sigma r}$ compared to the mutual inductance L_m, the required parameters can be simplified as

$$K_\sigma \approx \frac{3}{2}\frac{1}{L_{\sigma s}+L_{\sigma r}}\cdot\frac{L_r}{L_m}=1+\frac{L_{\sigma s}}{L_m}\approx 1 \tag{26}$$

It can be seen from eq. (26) the deviation of L_m has little effect on k_σ and $\frac{L_r}{L_m}$ therefore, its influence on the performance of the proposed control scheme would also be immaterial.

4. SIMULATION RESULTS

The planed scheme for the doubly fed induction generator based system is shown in Figure 8, implemented by using MATLAB/Simulink and the results are presented. The rating of the DFIG is 2 MW and the values of the parameters are shown in the Appendix B, the dc link voltage of the converter is kept at 1200V. This PCD scheme controls the stator's Active and Reactive power from the rotor side converter. The duration of time period used in the results are 250 microseconds which gives the switching frequency of 2 KHz of the rotor side converter and the grid side converter keeps the DC link voltage to a constant value and it is controlled by dc voltage controller in a VSC transmission system with the same 2KHz frequency as shown in the Figure 8, to reduce the harmonics produced by the converters used in this scheme an AC high frequency filter is used in the stator side.

For the PWM modulator the desired value of the rotor controlling voltage is then calculated and passed through it. Normally in our practical systems currents and voltages are set for the starting of the sampling period. There is a difference between the PWM modulator's and instantaneous sampling periods in the time periods in the control voltages of the rotor. In this PCD scheme the voltages in the rotor are calculated easily and the delaying of time instants should be considerably less, and it should be up to 50 micro seconds and this values shows that it a practical system for PCD control Scheme. During the operation of this scheme the converter at the grid side are operated at the time of starting, so the DC link voltage of the converter. The stator of the doubly fed induction generator will get the supply and gets energized with the constant rotor speed.

The dynamic outputs of this PCD scheme were tested with different values of the active and reactive powers. The outputs of the rotor speeds for the values of 1.0 to 1.2 per units are shown in the Figure 9 (A) and (B), where N_s is taken as reference and it is set to be 1 unit. The starting values of active and reactive powers for the stator was started at 0.2 seconds at rotor side converter and values taken as −2 Megawatts and −0.5 Mvar respectively, the values of powers at 0.4 seconds −2 to −1 Megawatts and at 0.6 seconds −05 to +0.5 Mvar's respectively. The efficient outputs of this scheme are shown in Figure 9. The dynamic outputs of both active and reactive powers are in few sec. There are no overlapping and overshoots in both the stator and rotor currents, active and reactive powers.

The harmonics generated in this scheme are shown in Figure 10 (a) and (b) and are called as harmonic spectra. These harmonics are for the stator and rotor currents are dominant at a frequency of 2 KHz. The harmonic spectra for different values of stator and rotor currents, powers are given in Figure 9 and 10.

The mutual Inductance is used in the controller having the values of 0% and 20% variations of desired outputs are given in Figure 11 (a) and (b), the rotor speed changes from 0.8 to 1.2 per unit at a time of 0.3 to 0.7 sec. Different values of power steps are given to active and reactive reference frames at 0.4 seconds −2 to −1 Megawatts and at 0.6 seconds −05 to +0.5 Mvar's respectively. Even in the large variations in the values of the inductances the PCD scheme gives a fine output responses in the Steady state and transient conditions, there is no change in the outputs when we compare the Figure 11 (a) and (b) and the response is acceptable.

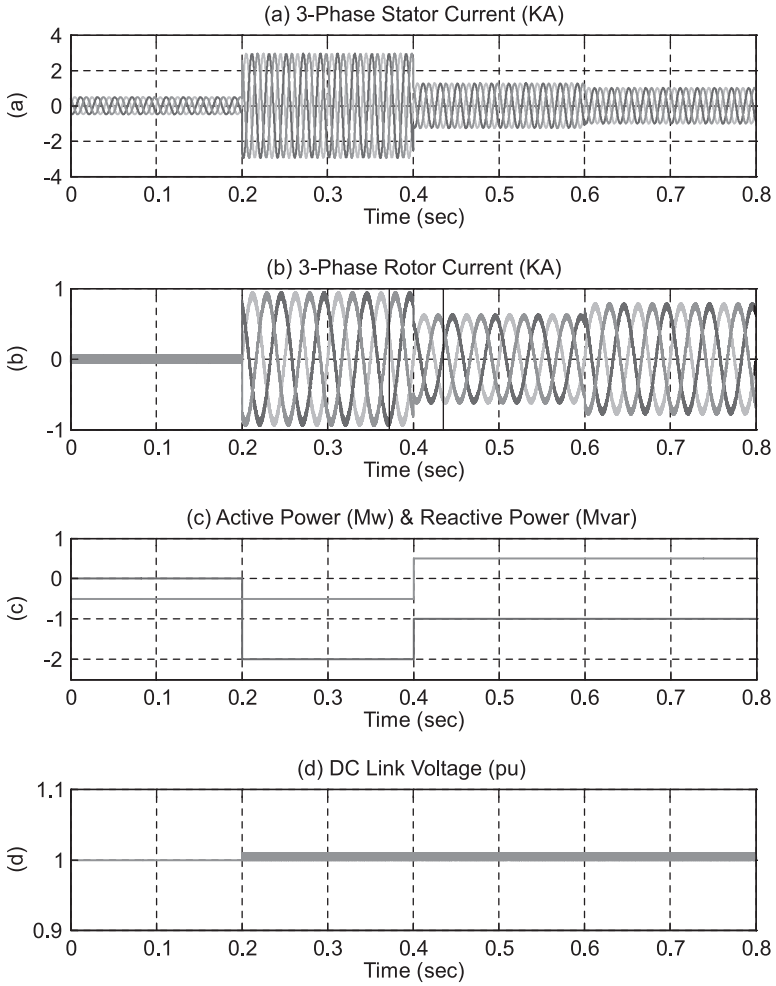

Figure 9: (A) At Rotor angular speed: 1.0pu; Time in (s)

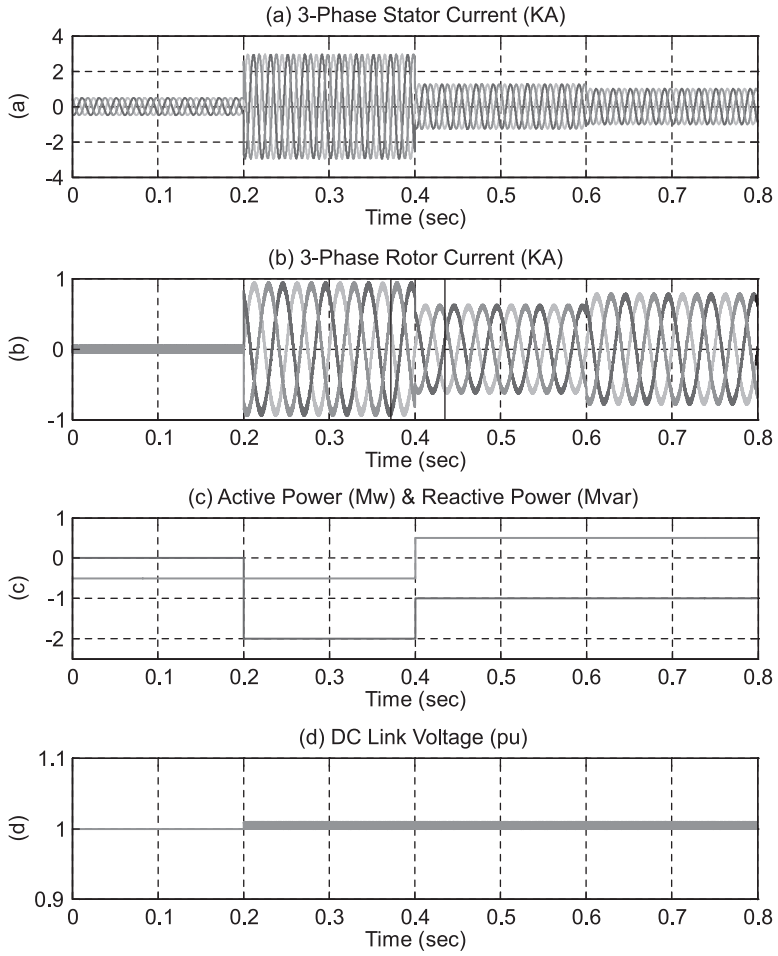

Figure 9: (B) At Rotor angular speed: 1.2pu; Time in (s)

Figure 9 performance of DFIG based generation system under various stator active and reactive power steps at constant rotor speed.

In a practical system voltages and currents are sampled at the start of the sampling time. The required rotor control voltage for the sampling time is then, calculated and passed to the PWM modulator. Predictably, there is a time delay between the instantaneous sampling and PWM modulator's receiving the required rotor control voltage. The proposed PCD scheme's rotor voltage calculation is relatively simple, and the time delay should be fairly small .though the simulated output rotor voltage is delayed by 50micro sec to closely represent a practical PCD control system. During the simulation, the grid side converter is enabled first. Such that the, converter dc link voltage is regulated. The DFIG stator is then, energized with the rotor rotating at a fixed speed, and with the rotor-side convertor disabled.

Initial studies with various active and reactive power steps were carried out to test the dynamic response of the proposed PCD scheme. The DFIG was assumed to be in speed control i.e., with the rotor speed set externally, since in a practical system, the wind turbines large inertia results in slow rotor speed change. Simulated results are shown in Figure 9 (A) and (B) for rotor speed of 1.0 and 1.2 pu, respectively, where the synchronous speed is defined as 1 unit. The rotor side was enabled at 0.2 sec with the initial stator active and reactive power references being –2 MW and –0.5 M var, respectively these active and reactive power references were step changed from. –2 to –1 MW at 0.4s and from –0.5 to 0.5 M var at 0.4 s respectively. The effectiveness of the planed control scheme is clear indicated in Figure (9). The dynamic response of both active and reactive powers is within few milliseconds. The step change of one control variable i.e., active and reactive power, does not affect the other due to the way the rotor voltage limit was applied. There is a no overshoot of either the stator/rotor currents or the active/reactive powers.

Studies with various power steps during rotor speed and machine parameter variations were carried out to further test the proposed PCD schemes Figure 10(A) and (B) shows the simulations with the mutual inductance used in the controller having 0% and 20% errors respectively. As shown during the period of 0.3 – 0.7 sec, the rotor speed increased from 0.8 to 1.2 pu. Various power steps were applied, i.e., active and reactive power references were changed from –2 to –1 MW at 0.4s and from –0.5 to 0.5 M var at 0.4 s, respectively.

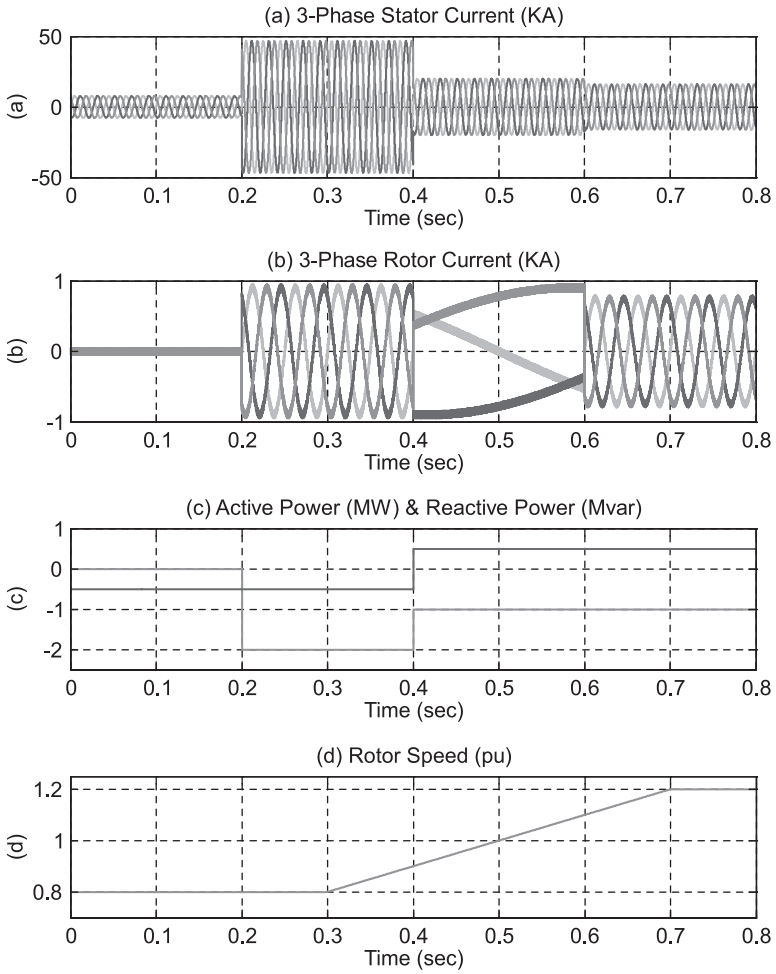

Figure 10: (A) with Normal L_m

Figure 10 Performance of DFIG based wind generation system under various stator active and reactive power steps and rotor speed variation.

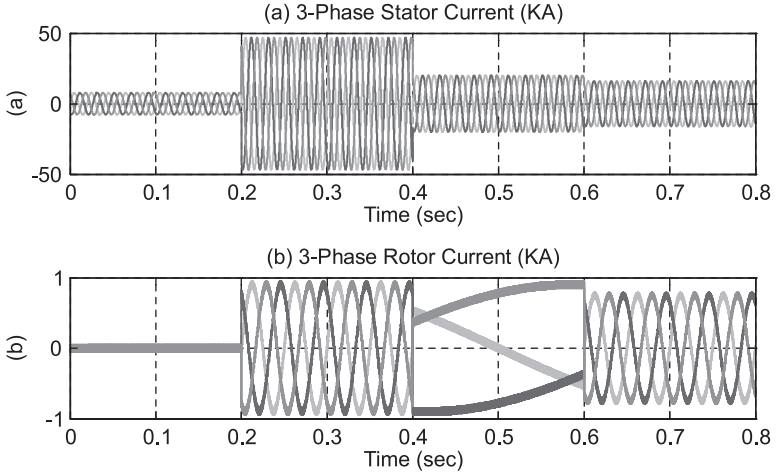

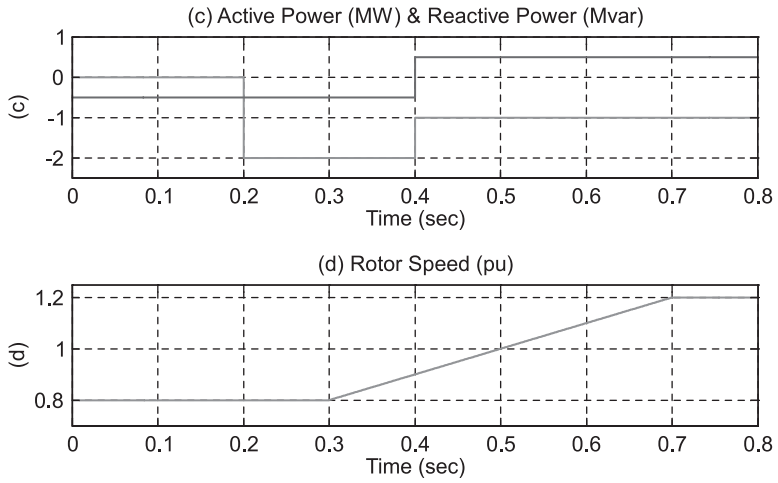

Figure 10: (B) with 20% L_m

As seen in Figure 10 (A) the system response with rotor speed variation is satisfactory. Comparing Figure 10 (A) and (B), the system maintenance superb performance under both steady state and transient conditions.

The proposed PCD robustness also tested with grid –side converter performance degraded to introduce significant dc voltage variation during transients. The effect of such a dc voltage variation on the dynamic and steady-state performances of the proposed PCD scheme is insignificant. Further tests for a complete generation system including a typical 2 MW wind turbine and DFIG were carried out. The DFIG was set in torque control the speed is the result of stator/rotor voltage/current and mechanical torque. The active power reference for the DFIG was calculated from the maximum power tracking curve [4], Figure 11 shows the simulated results when wind speed changes from 11 m/s to 13 m/sat 0.5 sec, and then to 10 m/s at 1.5 sec. The lumped inertia constant of the system is set to a relatively small value of 0.2 s in the study to decrease the simulation time. As can be seen from Figure 11, the system operation is reasonable and maximum power tracking is attained during wind speed variation.

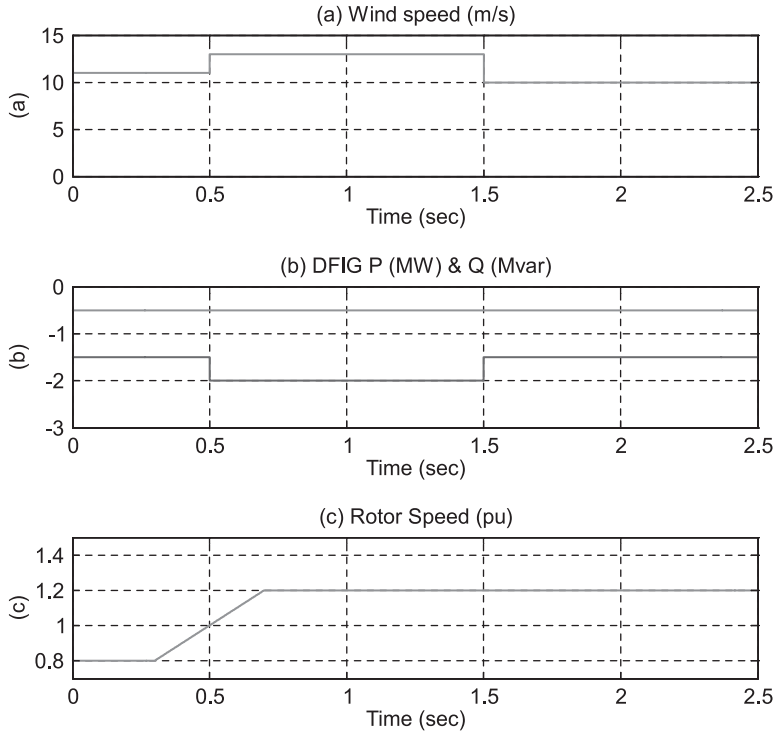

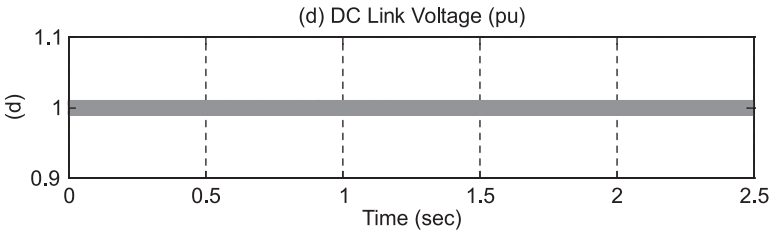

Figure 11: Performance of DFIG based wind generation system for step change of wind speed

Table 1
Parametrs of the Simulated DFIG

Rated Power	2 MW
Stator voltage	690 V
Stator turns ratio	0.3
R_s	0.018
R_r	0.0121 pu (ref to stator
L_m	3.362
$L_{\sigma s}$	0.102 pu
$L_{\sigma r}$	0.11 pu (refer to stator side
Lumped Inertia constant	0.2s
Number of pole pairs	2

5. CONCLUSION

The Active and Reactive power controlled scheme for a doubly fed induction generator based wind power generation system is presented in this paper. This scheme gives the rotor control voltage within the given duration by the stator flux, rotor positions and the values of the errors of the Active and Reactive powers. To improve the system Transient response by controlling the rotor voltage by using the low power ratings of rotor side converters. This converter constant switching frequency is used to attain the comfort of design and reduce the AC harmonics also. The effects of parameter variations of the response of the planed system are analyzed and are to be neglecting. This simulation results in more efficient conditions for the operation of the system and gives effectiveness of the parameters variations of the machine.

Appendix

A. Parameters effect the rotor voltage vector calculation: Considering $L_{\sigma s} << L_m$ and $L_{\sigma r} << L_m$, the constant $k\sigma$ and $\frac{L_r}{L_m}$ can be simplified as

$$K_\sigma = \frac{3}{2}\frac{1}{L_{\sigma s} + L_{\sigma r}} \tag{A1}$$

$$\frac{L_r}{L_m} = 1 + \frac{L_{\sigma s}}{L_m} \approx 1 \tag{A2}$$

B. Parameters of the DFIG used for simulation: See Table I for listing of the DFIG Parameters.

References

1. R. Pena, J.C. Clare, and G.M. Asher, "Doubly fed induction generator Using back-to-back PWM converters and its application to variable-speedwind-energy generation," I*nst. Elect. Eng. Proc. Elect. Power Appl.*, Vol. 143, No. 3, pp. 231-241, May 1996.
2. H. Akagi and H. Sato, "Control and performance of a doubly-fed induction Machine intended for a flywheel energy storage system," *IEEE Trans. Power Electron*., Vol. 17, No. 1, pp. 109-116, Jan. 2002.
3. R.W. De Doncker, S. Muller, and M. Deicke, "Doubly fed induction Generator systems for wind turbines," *IEEE Ind. Appl. Mag*., Vol. 8, No. 3,pp. 26-33, May/Jun. 2002.
4. Y.S. Lai and J.H. Chen, "A new approach to direct torque control of induction motor drives for constant inverter switching frequency and torqueripple reduction," *IEEE Trans. Energy Convers*., Vol. 16, No. 3, pp. 220-227, Sep. 2001.
5. N.R.N. Idris and A.H.M. Yatim, "Direct torque control of induction Machines with constant switching frequency and decreased torqueripple," *IEEE Trans. Ind. Electron*., Vol. 51, No. 4, pp. 758-767, Aug. 2004.
6. J. Kang and S. Sul, "New direct torque control of induction motor for Minimum torque ripple and constant switching frequency," *IEEE Trans. Ind. Appl*., Vol. 35, No. 5, pp. 1076-1082, Sep./Oct. 1999.
7. T. Noguchi, H. Tomiki, S. Kondo, and I. Takahashi, "Direct power control of PWM converter without power-source voltage sensors," *IEEE Trans.Ind. Appl*., Vol. 34, No. 3, pp. 473-479, May/Jun. 1998.
8. G. Escobar, A. M. Stankovic, J. M. Carrasco, E. Galvan, and R. Ortega, "Analysis and design of direct power control (PCD) for a three phase synchronous rectifier via output regulation subspaces," *IEEE Trans. Power Electron*., Vol. 18, No. 3, pp. 823-830, May 2003.
9. M. Malinowski, M.P. Kazmierkowski, S. Hansen, F. Blaabjerg, and G.D. Marques, "Virtual-flux-based direct power control of three-phase PWM rectifiers," *IEEE Trans. Ind. Appl*., Vol. 37, No. 4, pp. 1019-1027, Jul./Aug. 2001.
10. L. Xu and P. Cartwright, "Direct active and reactive power control of DFIGfor wind energy generation," *IEEE Trans. Energy Convers*., Vol. 21, No. 3, pp. 750-758, Sep. 2006.